Journal of Power Sources 268 (2014) 752–757

Contents lists available at ScienceDirect

Journal of Power Sources

journal homepage: www.elsevier.com/locate/jpowsour

Short communication

Near net shape manufacturing of planar anode supported solid oxide fuel cells by using ceramic injection molding and screen printing☆

R. Kluczowski*, M. Krauz, M. Kawalec, J.P. Ouweltjes

Institute of Power Engineering Ceramic Department CEREL, 1 Techniczna St., 36-040 Boguchwała, Poland

HIGHLIGHTS

- We prepare near net shape planar SOFCs with injection molded support layers.
- Functional layers are deposited by means of screen printing.
- The maximum power output is 1.25 W cm^{-2} at 800 °C, using hydrogen and air.

ARTICLE INFO

Article history:
Received 6 February 2014
Received in revised form
15 May 2014
Accepted 23 May 2014
Available online 7 July 2014

Keywords:
Solid oxide fuel cell
Ceramic injection molding
Near net shape
Economic viability

ABSTRACT

Ceramic injection molding is an economically and environmentally interesting technique to produce the support layers for anode supported solid oxide fuel cells. We investigated if this technique can be used for the support layer of manufacturing of planar AS–SOFCs in sizes of 50 × 50 and 100 × 100 mm^2. After setting the injection molding parameters, we could make 60 near net shape substrates per hour under semi-automatic conditions. Screen printing was used to apply the Ni–YSZ anode functional layer, 8YSZ electrolyte, 10GDC barrier layer and LSCF cathode. An electrochemical test on a 50 × 50 mm^2 cell revealed a maximum power density of 1.25 W cm^{-2} at 800 °C. SEM investigations have shown that the injection molded support layer adheres well to the screen printed anode functional layer, and that the anode support layer possesses a homogeneous microstructure. This shows that ceramic injection molding is a viable technique to economically produce planar AS–SOFCs at industrial scale.

1. Introduction

In order to produce anode supported solid oxide fuel cells (AS–SOFCs) in large quantities it is attractive to use fast, cheap and continuous production methods. For the deposition of thin layers (thickness generally below 50 microns) an economic and effective method is screen printing. For the preparation of thick layers like the support layer of AS–SOFCs, tape casting is the commonly used method because it is inexpensive and doesn't require complicated elements and tools [1–3]. But when it comes to large scale production this method is hardly effective. For example, in the case of using non-aqueous solvents, the time that is needed to obtain approximately 1 mm thick ceramic foil takes five to seven days. This is true for both batch tape casting and continuous tape casting. The usage of water based binder systems for tape cast foils, which have a clear advantage over non-aqueous binder systems from environmental perspective, require even longer processing time because of the relatively low evaporation rate of water [4–7]. A method that could significantly shorten the production time of the support layers for AS-SOFCs at potentially low costs and with low environmental impact is ceramic injection molding (CIM). This technique allows for the manufacturing of complex three dimensional parts with tight dimensional tolerances. Cost-intensive post-processing can frequently be avoided, which enables economical mass production of ceramic components [8]. Unfortunately, until recently CIM did not provide the tight tolerances and high repeatability that is required for many applications. Achieving precise dimensional control has been difficult for CIM because the injection molding process could easily give rise to problems such as powder-binder separation and particle orientation effects in the thermoplastic melt due to the high shear rates during the injection molding, incomplete cavity filling of complex parts, and anisotropic mechanical properties and shrinkage [9–14]. First attempts to use ceramic injection molding to obtain SOFC anode supports using this method were made by Panahi et al. [15]. Other work in this field

☆ This work was presented during the 4th Polish Forum Smart Energy Conversion and Storage, Krynica, Poland 1-4.10.2013.

* Corresponding author.
E-mail address: kluczowski@cerel.pl (R. Kluczowski).

http://dx.doi.org/10.1016/j.jpowsour.2014.05.132
0378-7753/

was conducted by Faes et al. and covered production of planar SOFC anodes including flow channels [16]. In both cases, the surface area of the anode supports did not exceed 20 cm^2. We have investigated if ceramic injection molding can be used for the production of planar AS-SOFCs with square geometry and dimensions of 50 × 50 and 100 × 100 mm^2 with a support thickness of 1 mm. The supports were made in-house by means of high-pressure injection molding. The thin layers were applied by a semi-automatic screen printer, while batch furnaces were used for sintering. The prepared AS–SOFCs were validated by means of geometrical characterization, their mechanical properties, and their electrochemical performance.

2. Experimental

For the preparation of anode supports a mixture of nickel oxide NiO (JT Baker) and yttria stabilized zirconia 8YSZ (TOSOH) were used in a ratio of 66:34 wt.%. To this powder mixture, 20 vol.% graphite powder (Carbon Polska) was added to serve as pore former during the sintering process. The mixture of nickel oxide, yttria stabilized zirconia and graphite powder was milled in a ball mill for 6 h with isopropanol as milling medium. After drying the slurry in a vacuum dryer at 70 °C, 10 wt.% thermoplastic binder (Zschimmer&Schwarz) was added by a mechanical stirrer in a heated chamber that was kept at 120 °C. This mixture was then granulized with a technologic line for pellets production. The line consists of a counter-rotating twin-screw compounder (Thermo Fisher), cooling bath and pelletizer (CEzEL). Anode supports were obtained by using both a BOY XS injection molding machine and Sumitomo Demag 60-310 injection molding machine, both with the following injection setting parameters:

- molding temperature: 110 °C
- cylinder temperature: 40 °C
- molding pressure: 1800 bar

The injection was provided in a horizontal way by means of a two-part water-cooled mold made of hardened tool steel. The obtained substrates were 62 × 62 mm^2 (BOY XS) and 125 × 125 mm^2 (Sumitomo Demag) in size.

Before the amount of thermoplastic binder and optimal parameters of injection were set, defects were observed in the injection molded substrates such as heterogeneity, deformation, cracks and cavities at the surface and in the bulk. Approximately 70 iterations were needed before the right injection molding parameters and the proper amount of binder (10 wt.%) were established. After setting the parameters of the injection molding less than 5% of substrates had defects. The reproducibility of the anode substrate was 95% with a production rate of 60 pieces per hour in the case of 62 × 62 mm^2 substrates and 60 pieces per hour in the case of 125 × 125 mm^2 substrates. The obtained substrates that passed visual inspection did not require any post processing. One particular advantage turned out to be possibility to reuse the substrates that had insufficient quality. It was shown that the mass could be reused six times without observing a decline in visual quality and repeatability.

In order to assess the economic advantages of injection molding over tape casting, the production capacities for both techniques were compared. With a production rate of 60 substrates under semi-automatic conditions and a size of 125 × 125 mm^2 it would imply that within 24 h it is possible to obtain 22.5 m^2 of anode supports by means of injection molding. While in the case of continuous tape casting, under the assumptions that this tape caster has an effective width of 100 cm and operates at a tape casting speed of 1.3 cm min^{-1}, only 18.7 m2 substrate area would be obtained. Furthermore, such continuous tape caster would demand huge area, for example 20 m of length with a casting speed of 1.3 cm min^{-1} and 24 h drying time. It shows that injection molding method is more effective and economic than tape casting method.

The qualified injection molded substrates were then heated in an electric furnace with debinding system HT 64/17 HDB (Nabertherm) at a temperature of 1100 °C for 1 h to remove the organics. Subsequently, the anode functional layer, anode contact layer and electrolyte layer were applied by means of a semi-automatic screen printer type KPX 2012. The anode functional layer consisted of NiO (JT Baker) and 8YSZ (TOSOH) powder mixture in a 1:1 weight ratio. The anode contact layer, which was applied at the counter-side of the substrates, consisted of NiO (JT Baker). The electrolyte layer consisted of 8YSZ (TOSOH). All screen print pastes were prepared in a planetary mill during half an hour with proper organic medium, and included ethylcellulose (Fluka) to serve as binder, while bis(2-ethylhexyl)phthalate (Merck) and tixatrol (Elementis) were added to, respectively, serve as plasticizer and to improve the thixotropy (i.e. shear thinning property) of the screen print pastes. Terpineol (Merck) was used as solvent and dispersant. After applying the thin ceramic layers, the substrates were sintered at 1400 °C for 3 h. The electrolyte was then coated with a gadolinia doped ceria layer $Ce_{0,9}Gd_{0,1}O_{1,95}$ 10GDC (Praxair) by screen printing. This layer, which was applied to serve as a so-called barrier layer, i.e., to prevent chemical reaction between the electrolyte and the cathode, was sintered at 1350 °C for 1 h. Finally, a lanthanum strontium cobalt ferrite perovskite $La_{0,6}Sr_{0,4}Co_{0,2}Fe_{0,8}O_{3-\delta}$ (LSCF, Praxair) cathode layer was applied on the sintered 10GDC layer by screen printing. This LSCF layer was sintered at 1100 °C for 1 h.

After the production stage of the AS–SOFCs the electrical characteristics and microstructural properties were investigated. The electrical properties were investigated at FCH Test Center in Denmark, using nickel mesh for anode current collection and gold mesh for cathode current collection. The cell was sealed at both the anode and cathode side by means of a high temperature steel frame sandwiched between glass felts. Flow distribution was accomplished by means of parallel flow channels provided in the ceramic cell housing. The test included 48 h conditioning at constant electric load at 800 °C. After the 48 h period additional measurements were performed in order to interpret the electrochemical results. A more extensive description of the test can be found here:

- Heat the cell to 900 °C, using 500 ml min^{-1} nitrogen at the anode side and 500 ml min^{-1} air at the cathode side
- Reduce the anode by replacing the 500 ml min^{-1} nitrogen with 500 ml min^{-1} hydrogen humidified at ambient temperature
- Change cathode flow to 2000 ml min^{-1} air
- Change anode flow to 1000 ml min^{-1} hydrogen humidified at ambient temperature
- Cool the cell to 800 °C
- Measurement of polarization curve
- Conditioning for 48 h at 1 A cm^{-2}
- Measurement of polarization curve and four-point electrochemical impedance spectroscopy (EIS) measured at 3 different current loads, both performed at 3 temperatures (750 °C, 800 °C and 850 °C) and using 3 different combinations of electrode gases. The impedance spectroscopy measurements were carried out between 0.0545 Hz and 96850 Hz with 12 steps per decade, using an integration time of 200 s between 96,850 and 6.7 Hz, an integration time of 60 s between 6.598 and 0.67 Hz, and an integration time of 36 s between 0.6598 and 0.05 Hz. The oscillation current was 60 mA [17].
- Change cathode flow to 500 ml min^{-1} air

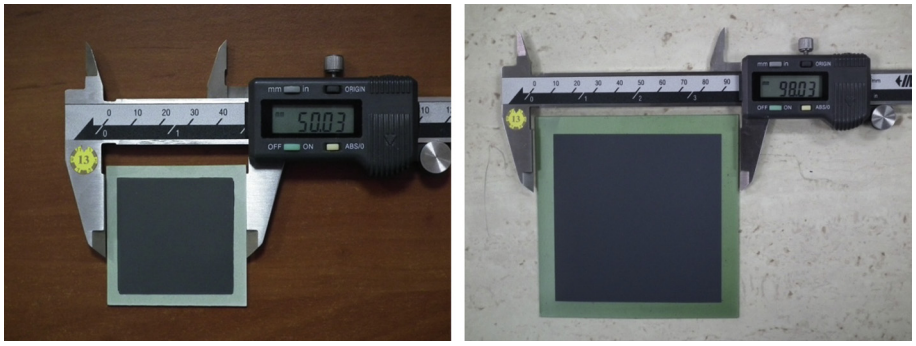

Fig. 1. AS–SOFC with dimensions 50 × 50 mm^2 (left) and 100 × 100 mm^2 (right).

– Change anode flow to 72 ml min^{-1} hydrogen + 728 ml min^{-1} nitrogen humidified at ambient temperature
– Cool the cell to room temperature

The sample that was used for the electrochemical test was analyzed by means of a scanning electron microscope type Hitachi ES-3400N.

3. Results

Fig. 1 shows typical examples of anode supported solid oxide fuel cells with final dimensions of 50 × 50 mm^2 and 100 × 100 mm^2, respectively. Both kinds of cells were flat without any local deformation and surface defects. The measured open porosity, which was determined by means of a hydrostatic method, of the sintered anode substrates (oxidized state) was 23 vol. %.

An overview of the electrochemical test can be found in Fig. 2. A detailed view of the cell voltage stability while the sample was operated at 1 A cm^{-2} galvanostatic load can be found in Fig. 3. It can be seen that the cell voltage declined during operation at 1 Acm^{-2}. Later during this test, a voltage decline was observed while the cell was kept at open circuit conditions at 650 °C (Fig. 2). This decline, that started after 230 h operation, was caused by partial short-circuiting of the test sample in the fuel cell test-rig at the FCH Test Center. The short-circuit disappeared after reheating the sample to 800 °C, most likely due to slight movement of the sensing wires upon heating.

The maximum power density that was obtained at 800 °C was 1,25 W cm^{-2} (Table 1, Fig. 4). Each measurement point in Fig. 4 was obtained after temperature equilibration. This was needed to compensate for the increasing Joule heat after each current increment. The measurement results obtained at 850, 750 and 650 °C show that the power output decreases with decreasing temperature. This is a common effect for solid oxide fuel cells, as the ohmic losses increase while the overall electrode kinetics slow down when the operating temperature is reduced. Further, it can be seen that the OCV obtained at 800 °C is substantially higher than the OCV at 750 °C, while the Nernst equation predicts opposite behavior. This is probably related to the higher fuel flow used during the measurements at 800 °C, which helped to suppress air backflow at the anode side that could exist due to imperfect gas sealing. A comparison of the measured cell performance with literature data is difficult, as the performance may depend largely on the test conditions. It can however be stated that the performance characteristics obtained at 650, 750 and 850 °C are comparable to those obtained by Birkl, who measured his anode supported cells in the same test equipment and under the same conditions [17].

Fig. 5 shows a selection of the impedance spectroscopy measurements that were carried out at 800 °C. It can be observed that the high frequency intercept with the *x*-axis, which is an indication

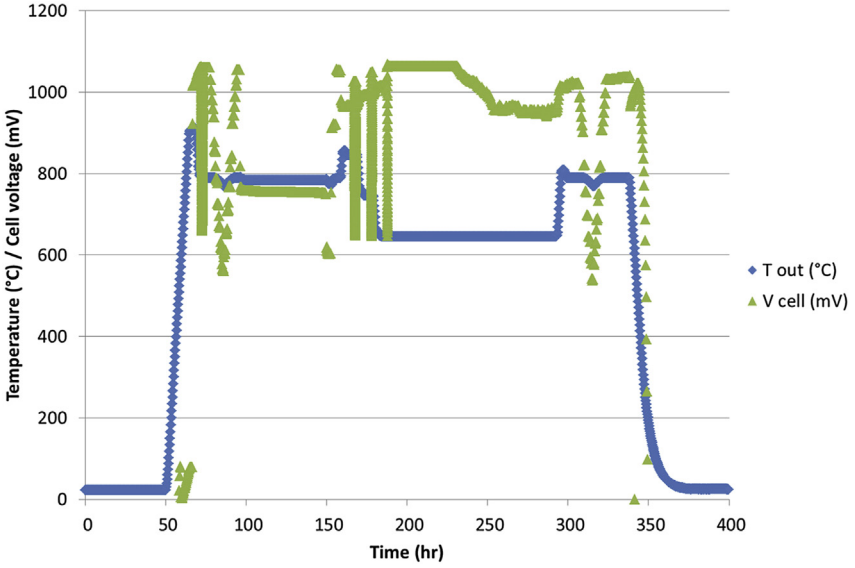

Fig. 2. Overview of the electrochemical test on a 50 × 50 mm^2 cell.

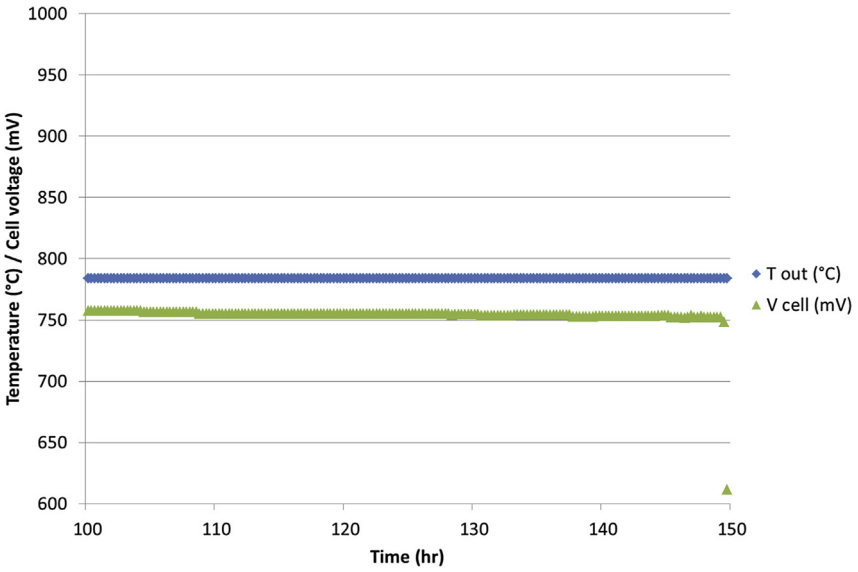

Fig. 3. Detailed view of the electrochemical test during the 48 h period at 1 A cm^{-2} galvanostatic load at 800 °C.

Table 1
Open circuit voltage (OCV), maximum power density and related fuel utilization (UF) of the tested sample between 650 and 850 °C. Note that the results at 800 °C were obtained at different gas flows than those at 850, 750 and 650 °C.

Time [hr]	Temperature [°C]	OCV [mV]	Power density [W cm^{-2}]	Fuel flow [ml min^{-1}]	UF at maximum power density [%]	Oxidant flow [ml min^{-1}]
76	800	1061	1.25	$1000H_2$	24	$420O_2 + 1580N_2$
167	850	1026	1.37	$400H_2$	58	$498O_2 + 1843N_2$
178	750	1048	0.77	$400H_2$	33	$498O_2 + 1843N_2$
188	650	1062	0.25	$400H_2$	10	$498O_2 + 1843N_2$

for the ohmic losses of the system, was more or less constant at 0.11 Ω cm^2. Furthermore, a sharp drop of the polarization losses with current load was seen. At OCV, the total polarization losses amounted 0.37 Ω cm^2. At 1.00 A cm^{-2} galvanostatic load the polarization losses had dropped to 0.26 Ω cm^2. And at 1.88 A cm^{-2}, only 0.10 Ω cm^2 polarization losses were observed. Interpretation of the polarization losses shown in Fig. 5 indicated three different processes. The obtained impedance spectra were compared with those reported in the literature [18,19]. From that it seems that the process responsible for the arc with a turnover frequency between 4 and 10 Hz is most likely related to the cathode, while the process with a turnover frequency ranging between 550 Hz at open circuit conditions and 4 kHz at maximum current density is most likely related to the anode. The third arc, which was only clearly visible at high current density and had a turnover frequency of 545 Hz, is most likely related to the cathode.

Fig. 6 shows the anode side of the sample after electrochemical testing. It can be observed that the central area of the cell has a gray

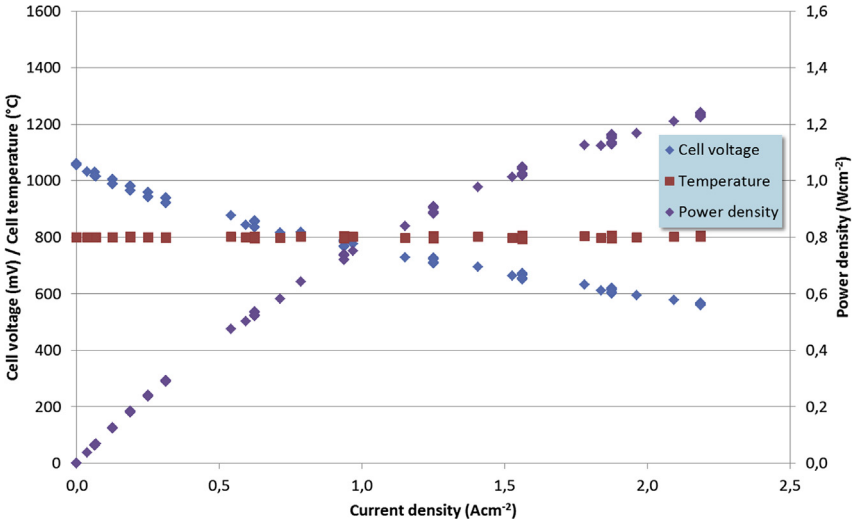

Fig. 4. I–V and I–P curve of the tested sample at 800 °C.

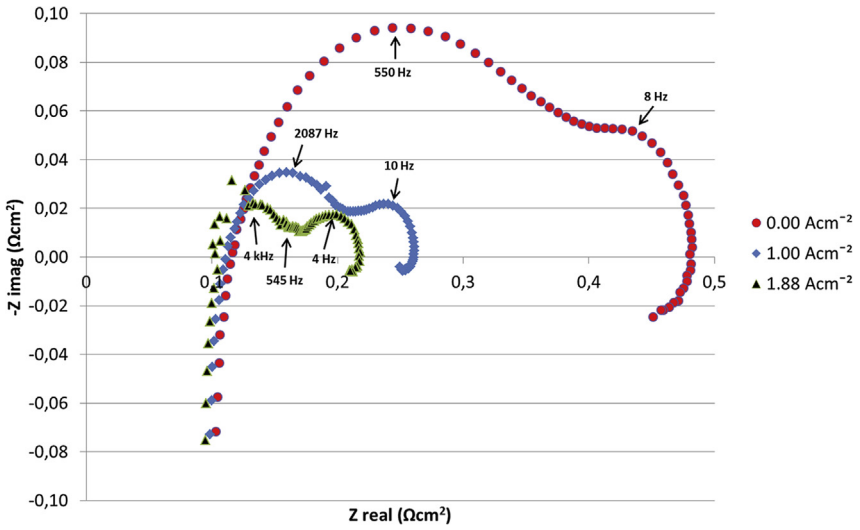

Fig. 5. Results from impedance spectroscopy measurements at 800 °C.

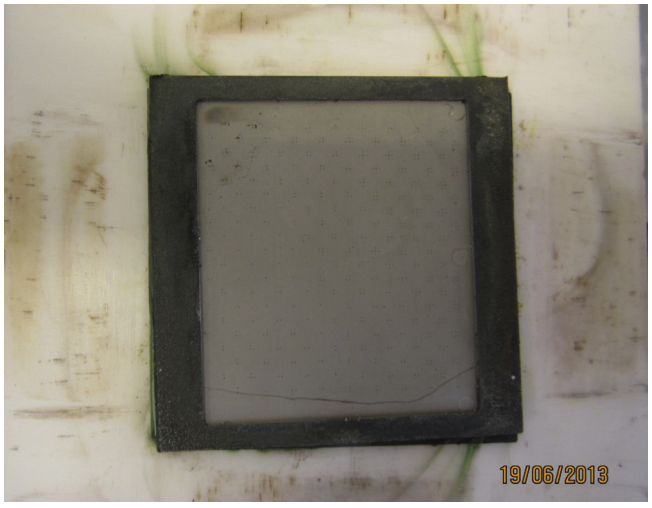

Fig. 6. Anode side of the tested sample after dismounting.

color, which indicates that the nickel in the anode is in metallic state, while the edges of the cell are green (in web version), which indicates that the nickel is oxidized to nickel oxide. Further, a crack can be observed in the gray area. There is no discoloring along the crack from gray to green (in web version). This indicates that the crack was formed at a temperature that does not promote oxidation to nickel oxide. The crack was caused because the cell was fixed to the alumina housing via glass sealing. The alumina housing has a lower thermal expansion coefficient than the cell, hence the cell cracks as the housing is much stronger. Hence, it did not affect the test results. Also, it can be seen that there is a gap between the frame and the cell to the left of the image. This is probably due to misalignment of the cell and the cathode frame. The reason for the misalignment is most probably due to the dimensions of the cell which is 50 × 50 mm^2 whereas the cells usually tested in the set-up at the FCH test center are 53 × 53 mm^2.

Figs. 7 and 8 show SEM images of polished cross sections of the tested sample. The SEM images show that the injection molded layer adheres well to the screen printed layers. This indicates that ceramic injection molding is a viable technique to produce the support layers for AS–SOFCs. Fig. 8 shows the interfaces between the functional layers in more detail. Good adherence between the anode functional layer, the electrolyte, the barrier layer and the cathode can be seen. The electrolyte has a thickness between 3 and 5 microns. This layer only exhibits enclosed pores and is thus thought to be gas tight. The 10GDC barrier layer, on the other hand, is still porous. This could give rise to increased electrical resistivity and reduced mechanical integrity. The anode functional layer and cathode layer appear to

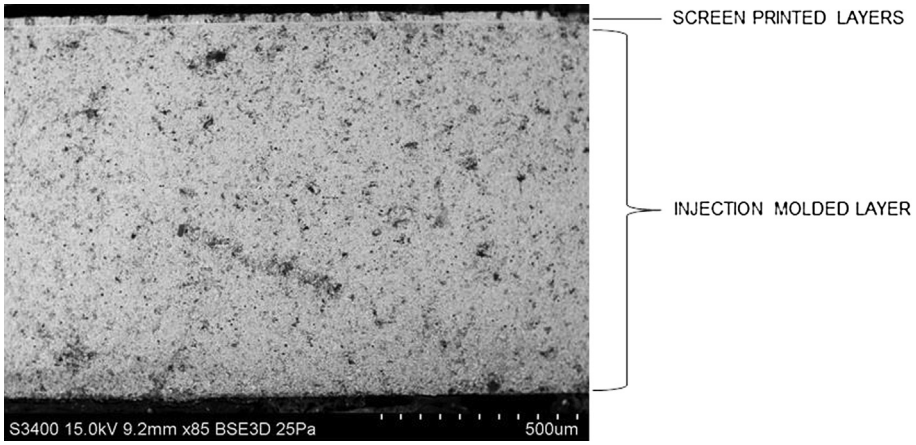

Fig. 7. Cross section of the tested sample (SEM 85x).

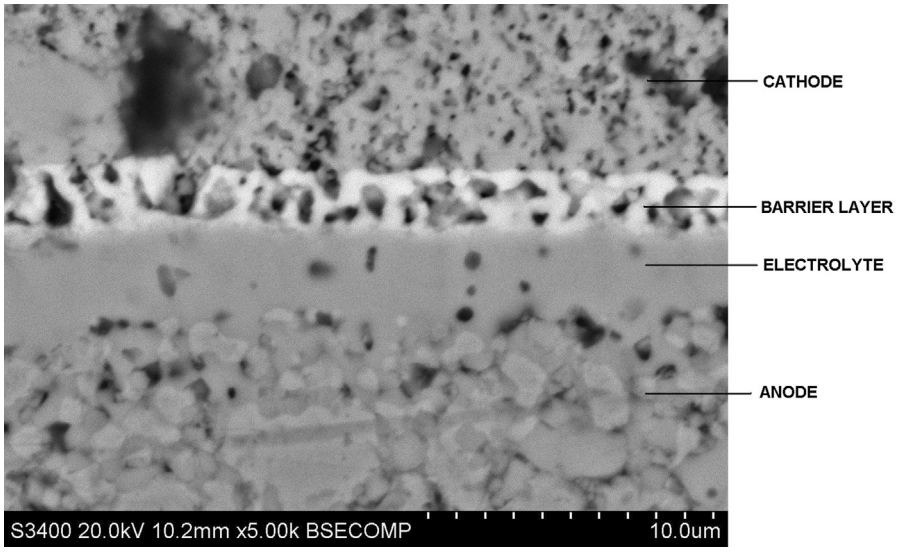

Fig. 8. Cross section of the tested sample (SEM 5000x).

possess sufficient open porosity for mass transport to the electrochemically active sites close to the electrolyte.

4. Conclusions

Our research has shown that ceramic injection molding is a viable process to produce planar anode supported solid oxide fuel cells with promising mechanical and electrochemical properties. This proves that this manufacturing method can be used to produce anode support layers for AS–SOFCs at industrial scale, with clear economic and environmental advantages over tape casting.

Acknowledgment

This work is supported by the Polish National Center of Research and Development, within the strategic project SP/E/4/65786/10 “Opracowanie zintegrowanych technologii wytwarzania paliw z biomasy, odpadów rolniczych i innych”. FCH Test Center in Denmark is gratefully acknowledged for measuring the electrical properties of the prepared AS-SOFC. This paper has been presented on the 4th Smart Energy Conversion and Storage Conference 1-4 October 2013 in Krynica, Poland.

References

[1] J. Will, A. Mitterdorfer, C. Kleinlogel, D. Perednis, L.J. Gauckler, Solid State Ionics 131 (2000) 79–96.
[2] Y. Zhang, Z. Lü, X. Huang, M. An, B. Wei, W. Su, J. Solid State Electrochem. 15 (2011) 2661–2665.
[3] A. Gondolini, E. Mercadelli, P. Pinasco, C. Zanelli, C. Melandri, A. Sanson, Int. J. Hydrogen Energy 37 (2012) 8572–8581.
[4] Z. Rak, R. Kluczowski, M. Krauz, Ceramika 96 (2006) 459–466.
[5] M. Krauz, R. Kluczowski, J. Trawczyński, R. Nowak, in: P. Da Costa, G. Djéga-Mariadassou, A. Krztoń (Eds.), Catalysis for Environment: Depollution, Renewable Energy and Clean Fuels: proceedings of the 2006 conference, Zakop, 20–23, Polish Academy of Sciences, Centre of Polymer and Carbon Materials, September 2006, pp. 123–127.
[6] M. Krauz, K. Krząstek, R. Kluczowski, in: J. Potencki (Ed.), XXXI International Conference of IMAPS Poland Chapter: Proceedings of the 2007 conference, Rzeszów-Krasiczyn, 23–26, International Microelectronics and Packaging Society, September 2007, pp. 503–506.
[7] T. Golec, M. Miller, R. Antunes, J. Jewulski, A. Klimov, M. Stepien, M. Krauz, R. Kluczowski, K. Krzastek, R. Nowak, J. Fuel Cell. Sci. Technol. 7 (2010), 011003–1-5.
[8] M.A. Sellés, S. Sanchez-Caballero, E. Perez-Bernabeu, Procedia Technol. 12 (2014) 439–441.
[9] S.M. Ani, A. Muchtar, N. Muhamad, J.A. Ghani, Cer. Int. 40 (2014) 273–280.
[10] T.S. Shivashankar, R.K. Enneti, S.-J. Park, R.M. German, S.V. Atre, Powder Technol. 243 (2013) 79–84.
[11] F. Sommer, H. Walcher, F. kern, M. Maetzig, R. Gadow, J. Eur. Ceram. Soc. 34 (2014) 745–751.
[12] J. Hidalgo, A. Jiménez-Morales, J.M. Torralba, J. Eur. Ceram. Soc. 32 (2012) 4063–4072.
[13] A. Mannschatz, A. Müller, T. Moritz, J. Eur. Ceram. Soc. 31 (2011) 2551–2558.
[14] P. Dvorak, Th. Barriere, J.C. Gelin, J. Eur. Ceram. Soc. 28 (2008) 1923–1929.
[15] A.K. Panahi, H. Khoshkish, M.R. Saraji, Ionics 17 (2011) 733–740.
[16] A. Faes, H. Girard, A. Zryd, Z. Wuillemin, J. Vanherle, J. Power Sources 227 (2013) 35–40.
[17] C. Birkl, Effects of Anode Sintering Temperature on Microstructure and Performance of Multilayer Tape Cast SOFC, MSc thesis, DTU Energy Conversion, Technical University of Denmark, September 2012.
[18] J.P. Ouweltjes, M. van Tuel, F. van Berkel, G. Rietveld, in: Electrical Efficiency and Electrochemical Stability of Cathode Supported Electrolyzers”, Proc. 9th European SOFC Forum, 2010 (Luzern).
[19] J.P. Ouweltjes, L. Berkeveld, B. Rietveld, in: D. Stolten, T. Grube (Eds.), 18th World Hydrogen Energy Conference 2010 – WHEC 2010, Parallel Sessions Book 3: Hydrogen Production Technologies – Part 2, Proceedings of the WHEC, May 16-21, 2010 (Essen), pp. 65–76.